The College of William and Mary

Undergraduate Senior Thesis

Measurement of the frequency shift parameter κ_0 in spin-polarized K-^{3}He collisions

Joshua Hill

Advisor: Dr. Todd Averett

Senior Research Coordinator: Dr. Henry Krakauer

A thesis submitted in partial fulfillment of the requirements for the degree of Bachelor of Science

Department of Physics

December 2013

Abstract

Electron scattering experiments studying the internal structure of the neutron require spin-polarized neutron-equivalent targets. ^{3}He nuclei are employed as a neutron substitute in these targets. Polarization (spin) is transferred to the ^{3}He nuclei via collisions with optically pumped alkali metal vapor atoms. Measurements of the ^{3}He's polarization are affected by uncertainty in a dimensionless parameter characterizing the quantum mechanical magnetic interaction between the alkali metal electrons and the ^{3}He nuclei. This parameter, κ_0, has not yet been directly measured for K, having been previously found indirectly via κ_0 for Rb. We constructed and implemented a polarization-insensitive experiment designed to directly measure κ_0 for K. This was done by measuring the K electron-paramagnetic-resonance (EPR), Zeeman frequency shift of a particular hyperfine (F, m_F) transition in the presence of spin-polarized ^{3}He. Using a cylindrical target oriented parallel, then perpendicular, to an applied magnetic field,we took a range of data on the difference in the EPR frequency measured between different target orientation. The two orientations will allow us to isolate the frequency shift due to the K-^{3}He quantum mechanical spin-exchange, from that of the classically magnetized ^{3}He, and thus to isolate the κ_0 of K. Our preliminary results, uncorrected for polarization losses inherent in each measurement indicate κ_0 values of the same order as those predicted by other groups; i.e. between 6 and 9. Efforts to correct for polarization losses, temperature gradients along the experimental target, and repeat-ability of the frequency shift measurements (EPR photodiode alignment) are underway, and will reduce the systematic uncertainty in our values.

Acknowledgements

I would like to thank Dr. Todd Averett, Nick Penthorn, Christine McLean, Elana Urbach, my mother Susan, my grandparent, the friends I have made at William and Mary, my teachers from Tomas Nelson Community College, and Baby (a very nice cat).

Symbols

SEOP	Spin Exchange optical Pumping
EPR	Electron Paramagnetic Resonance
NMR	Nuclear Magnetic Resonance
AFP	Adiabatic Fast Passage
RF	Radio Frequency
G	Gauss

D_2	Specific Frequency Light of Alkali Metal Energy Level Transition
P	^{3}He Polarization
$\boldsymbol{B_0}$	Holding (Primary) Magnetic Field
$\boldsymbol{B_1}$	Radio Frequency Magnetic Field
$\boldsymbol{B_M}$	Classically Magnetized ^{3}He Magnetic Field
$\boldsymbol{B_{SE}}$	Spin Exchange Frequency Shift Equivalent Magnetic Field
$\boldsymbol{K}$	^{3}He Nuclear Angular Momentum
$\boldsymbol{S}$	Alkali Metal Electron Spin Angular Momentum
$\boldsymbol{J}$	Alkali Metal Electron Total Angular Momentum
$\boldsymbol{I}$	Alkali Metal Total Atomic Angular Momentum
$[He]$	^{3}He Number Density
h ($\hbar$)	Standard (and Reduced) Plank's Constant
m_e	Mass of Electron
m_p	Mass of Proton
g_e	Alkali Metal Electron Spin g-factor
g_I	Alkali Metal Nuclear g-factor
g_J	Alkali Metal Electron Total Angular Momentum (Landè) g-factor
g_K	^{3}He Nuclear g-factor
F	Total Atomic Angular Momentum Quantum Number (Manifold)
m_F	Total Atomic Angular Momentum Magnetic Quantum Number
e	Fundamental Charge
$\boldsymbol{M}$	Magnetization

$C(\boldsymbol{x})$	^{3}He Target geometry Dependent Constant
K	Elemental Symbol for Potassium, magnitude of ^{3}He nuclear spin
A_{hf}	Hyperfine Coupling Constant
l	Electron Orbital Angular Momentum Quantum Number
S	Electron Spin Angular Momentum Quantum Number
J	Electron Total Angular Momentum Quantum Number
Γ_{SE}	Alkali Metal-^{3}He Spin Exchange Rate per Atom
$\langle v\sigma_{SE}\rangle$	Velocity Averaged Spin Exchange Cross Section
κ_0	Spin Exchange EPR Frequency Shift Parameter (Spherical Target)
κ_{SE}	Ratio of Real to Imaginary parts of σ_{SE}
κ_{eff}	EPR Frequency Shift Parameter (Non-spherical)
$\Delta\nu_{SE}$	EPR Frequency Shift Attributable to Spin Exchange
$\Delta\nu_M$	EPR Frequency Shift Attributable to Classically Magnetized ^{3}He
$\Delta\nu_{\parallel}$	EPR Frequency Shift When $\boldsymbol{B_0} \parallel \boldsymbol{B_M}$
$\Delta\nu_{\perp}$	EPR Frequency Shift When $\boldsymbol{B_0} \perp \boldsymbol{B_M}$
μ_B	Bohr Magneton
μ_K	^{3}He Nuclear Magnetic Moment
μ_N	Nuclear Magneton
μ_J	Electron Total Angular Momentum Magnetic Moment
α	Fine Structure Constant
Φ	EPR Frequency $\Longleftrightarrow$ Polarization Conversion Constant
ΔE_{hf}	Zero Magnetic Field Hyperfine Energy Splitting
η	Constant Characterizing Hyperfine Interaction
$\sigma_{\pm}$	Left or Right Circularly Polarized Light
γ	Gyromagnetic Ratio
τ	Torque
ω	Angular Frequency
ω_0	Larmor Frequency

Chapter 1

Introduction

Our lab produces, characterizes, and studies nuclear-spin-polarized targets made from an isotope of helium, "helium three", hearafter ^{3}He. The predominant use of many of the targets produced is in electron-scattering experiments studying the inner structure of the neutron at the Thomas Jefferson National Accelerator Facility (JLab) in Newport News, VA.

^{3}He is used as a stable, neutron substitute. In the ground state of ^{3}He, 88.2% of the nuclei are in a configuration (S-state) such that their two protons' spins are aligned antiparallel [1]. These spins cancel, leaving the net spin of the nucleus to be dictated by the remaining nucleon, the neutron with spin $\pm\frac{1}{2}$. Thus, from a spin-polarization point of view, ^{3}He is an effective neutron substitute. Here, polarization means the percentage of ^{3}He nuclear spins pointing in the same direction.

Most targets are approximately the size of a shoe box, and are pressurized. They are made of hollow glass, and filled with ^{3}He, N_2, and alkali metals. The N_2, and alkali metals, are required for the method we use to polarize the ^{3}He. The ^{3}He nuclei are polarized indirectly via Spin Exchange Optical Pumping, or SEOP, whereby:

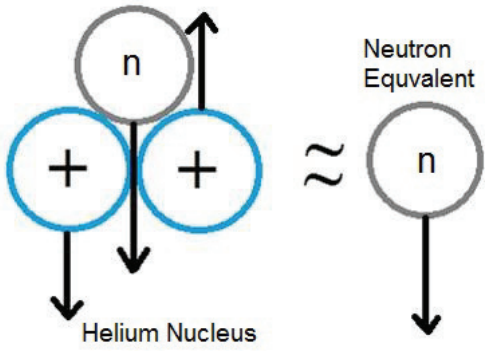

FIGURE 1.1: ^{3}He nucleus as a spin-substitute for a lone neutron.

1. Circularly polarized laser light enters the target, heated externally via forced-air.
2. Vaporized alkali metals' valence electrons become polarized (optical pumping)
3. Binary alkali metal-^{3}He collisions transfer the spin state to the ^{3}He nucleus, and thus the neutron (spin exchange).

We use an applied "holding" magnetic field ($\boldsymbol{B}_0$), to cause a Zeeman splitting in the energy levels of the alkali metals' electrons. Electron Paramagnetic Resonance (EPR) is then used to determine the frequency difference between the, now differentiated, alkali metal electron hyperfine energy levels. This frequency differs from that expected due to the holding field alone for two reasons. First, the bulk spin-polarized ^{3}He creates a classical magnetic field ($\boldsymbol{B}_M$), which influences the frequency shift. Second, the spin-exchange process itself causes a frequency shift, over and above that due to the bulk ^{3}He (spherical geometry), parameterized by the dimensionless constant κ_0 [5]. This spin exchange shift can be treated as being due an additional magnetic field ($\boldsymbol{B}_{SE}$), dependent upon the helium density and polarization [3]. κ_0 is specific to the particular alkali metal and alkali metal isotope in question.

Prior to 2005, the alkali metal used in the targets was Rb [9]. Now, however, a hybrid alkali metal mixture of K and Rb is used. The K relaxes (depolarizes) more slowly than Rb, and can act as a "reservoir" for the desired spin state. The K in conjunction to the Rb is more efficient at transferring spin to the ^{3}He, from the viewpoint of a photon [1]. Rb is maintained in the targets as current cost-affordable laser technology precludes directly optically pumping K. Because of the previous use of Rb in targets, κ_0 was determined for them, and has also been indirectly found for K (see table at end of report). However, previous values of κ_0 for K suffer from being obtained using the polarization of the ^{3}He and κ_0 for Rb, along with their associated uncertainties. Moreover, the previous values of κ_0 for K were found for temperatures below what is used in our lab at William and Mary, approximately 235°C.

It is important to reduce the uncertainty in κ_0 for K, as uncertainty in it introduces a proportional amount of uncertainty in the ^{3}He polarization. The polarization value is, in turn, used in nuclear physics experiments wherever the targets are ultimately end up.

Chapter 2

Origin of κ_0

Quoting K. Kluttz [1],"Because the spin-exchange contribution [to the EPR frequency shift] is difficult to calculate from theory, it is parameterized by the unitless quantity, κ_0..." While we use EPR to isolate the frequency shift due to the ^{3}He from that of $\boldsymbol{B}_0$, to determine κ_0 we must further differentiate between the contributions due to the above mentioned classical magnetism, and the shift due to spin-exchange.

As before, the spin exchange's contact interaction can be treated as an additional magnetic field [6]. The interaction is proportional to the dot product of the ^{3}He nuclear angular momentum $\boldsymbol{K}$ (hereafter called the "nuclear spin"), and the alkali metal electron spin $\boldsymbol{S}$. To be clear, the contact interaction is not physically another magnetic field. Beginning with the time evolution equation for the density matrix ρ describing the Rb atoms in a magnetic field, Romalis derives (2.1) in [3] as an approximate equivalent for the spin-exchange contribution to the EPR frequency shifts.

This spin exchange equivalent magnetic field is, ignoring the nuclear Zeeman splitting, given by:

$$B_{SE} = \frac{2K_z\kappa_{SE}\Gamma_{SE}\hbar}{g_e\mu_B} \tag{2.1}$$

where $\Gamma_{SE} = [He]\langle v\sigma_{SE}\rangle$ is the alkali metal-He spin-exchange rate per atom. The ^{3}He number density is [He], and $\langle v\sigma_{SE}\rangle$ is the velocity average of the spin exchange cross section (σ_{SE}).The Bohr magneton is $\mu_B = e\hbar/(2m_e)$, and the electron g-factor is g_e. Because the ^{3}He nuclear spins are polarized in the $\hat{z}$ direction, the ^{3}He nuclear spin is $\langle \boldsymbol{K}\rangle = K_z\hat{z}$. κ_{SE} is the ratio of the imaginary part of σ_{SE} to its real part [3].

Because $\boldsymbol{B_{SE}}$ is small compared to the holding field, typically about 0.05G vs 20G, we use the derivative of the frequency with respect to the magnetic field [3]:

$$\Delta\nu_{SE} = \frac{d\nu(F,m)}{dB}B_{SE} \tag{2.2}$$

where $\nu(F,m)$ is the frequency of the hyperfine transition of interest $(F,m) \rightarrow (F, m \pm 1)$. F is the quantum number characterizing the total alkali metal atomic angular momentum, $\boldsymbol{F} = \boldsymbol{I} + \boldsymbol{J}$. The nuclear angualr momentum is $\boldsymbol{I}$, while the electron total angular momentum is $\boldsymbol{J}$.

The magnetization of the ^{3}He produces a classical magnetic field that shifts the frequency. The field is proportional to the magnetization ($\boldsymbol{M_{He}}$) via C, a ^{3}He-cell geometry dependent constant. The frequency shift due to this field is:

$$\Delta\nu_M = \frac{d\nu(F,m)}{dB} \cdot B_{classical} = \frac{d\nu(F,m)}{dB} C[He]\mu_K P_{He} \tag{2.3}$$

where μ_K is the ^{3}He nuclear magnetic moment, and $P = K_z/K$ is the polarization. Combining both shifts we obtain, for a spherical sample:

$$\Delta\nu = \Delta\nu_{SE} + \Delta\nu_M = \frac{d\nu(F,m)}{dB}\frac{8\pi}{3}\kappa_0\mu_K[He]P_{He} \tag{2.4}$$

where we have now defined κ_0 to include κ_{SE}.

A spherical cell is characterized by κ_0 For other geometries:

$$\kappa_0 \rightarrow \kappa_{eff} = \kappa_0 + \frac{3}{8\pi}C(\boldsymbol{x}) - 1 \tag{2.5}$$

where $C(\boldsymbol{x})$ is the above mentioned geometric correction factor, and is constant inside the central region of a long cylinder [3].

Note that κ_0 assumes a spherical ^{3}He sample. If we used only $C = 8\pi/3$ for a classically magnetized sphere, ignoring the alkali metal-He spin exchange interaction, κ_0 would equal one. Thus that κ_0 is positive means it can be thought of an an attractive enhancement of the alkali electron's wavefunction to the ^{3}He nucleus [3].

We are making measurements of κ_0 for K, at the 235°C operating temperature in the lab at William and Mary. For these to be insensitive to polarization (P_{He}) and the κ_0 of Rb, we have used a cylindrical cell that can rotate with respect to the laser and holding field. That the measurement be independent of P_{He} is important because we only know the polarization up to any uncertainty in κ_0, the value we ultimately wish to determine.

Measurements of the frequency shift of a particular K hyperfine transition are found with the cylinder in two orientations. These orientations are parallel to, then perpendicular to, the holding field. Key to this procedure is that the polarization is the same in both orientations. First we take the longitudinal and transverse frequency shift measurements. Then, introducing polarization to frequency conversion factors allows us to preserve κ_0 in the equations, while

eliminating P_{He}. The cylindrical cell geometry is necessary because for a spherical cell, the frequency shift would be invariant under rotation, and both P *and* κ_0 would cancel.

The magnetic field inside a spherical cell, assuming uniform magnetization $\boldsymbol{M}$, is $B = \frac{8\pi M}{3}$. A cylinder magnetized parallel to it's axis produces a magnetic field of $B_{\parallel} = 4\pi M$, while one magnetized perpendicular to it's axis produces $B_{\perp} = 2\pi M$. The frequency shifts of a particular hyperfine m_F level of a specific alkali metal are given by:

$$\Delta\nu_{\parallel} = \frac{d\nu(F,m)}{dB}\mu_K[He]P_{He}\left[\frac{8\pi}{3}\kappa_0 + \left(4\pi - \frac{8\pi}{3}\right)\right] \tag{2.6}$$

$$\Delta\nu_{\perp} = \frac{d\nu(F,m)}{dB}\mu_K[He]P_{He}\left[\frac{8\pi}{3}\kappa_0 + \left(2\pi - \frac{8\pi}{3}\right)\right] \tag{2.7}$$

In the cylinder, the areas outside the central region about which it is rotated contribute to the frequency shift via the above classical fields. However, because these outside regions do not come into contact with the ^{3}He in the central region, they *do not* contribute to the spin-exchange equivalent field in the center [3].

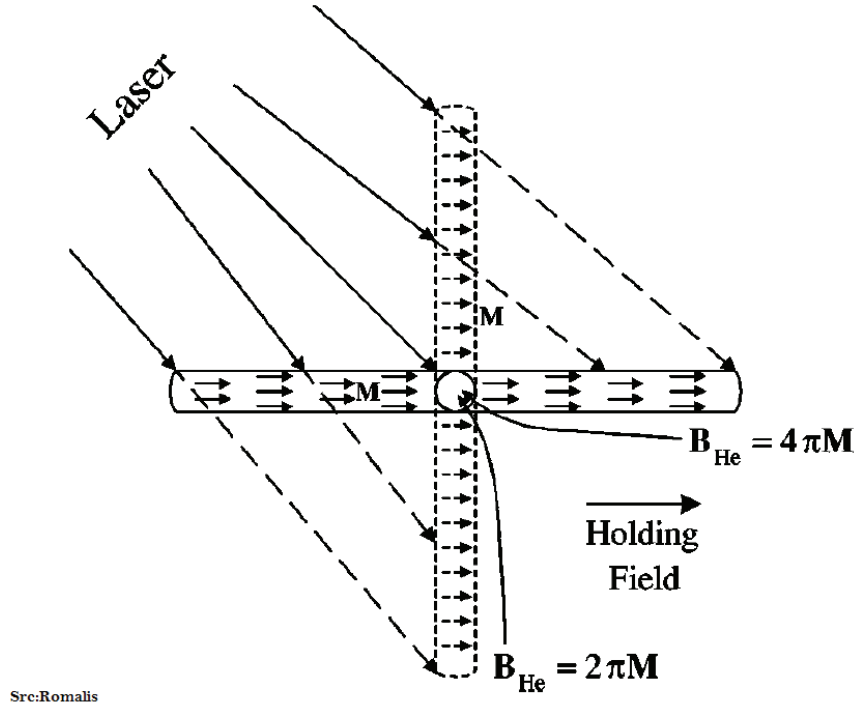

FIGURE 2.1: Cell orientations, and respective magnetization. The central circular region is not affected by B_{SE} of the outer pieces on either side.

If we then introduce the following polarization to frequency shift conversion factors $\Phi_{\parallel}$ and $\Phi_{\perp}$:

$$\Delta\nu_{\parallel} = P_{He}\Phi_{\parallel} \tag{2.8}$$

$$\Delta\nu_{\perp} = P_{He}\Phi_{\perp} \tag{2.9}$$

dividing (6) and (7) we obtain:

$$\kappa_0 = \frac{3}{8}\frac{(\Phi_{\parallel} + \Phi_{\perp})}{(\Phi_{\parallel} - \Phi_{\perp})} - \frac{1}{8} \tag{2.10}$$

where P_{He} cancels out in the first term.

κ_0 also appears to have a temperature dependence that was estimated to be linear by other groups, and is still being explored in our lab.

Chapter 3

Hyperfine Structure

3.1 Zeeman Effect

A magnetic moment dipole interacts with an external electric field by being subject to a torque τ which causes precession about the field. Therefore the moment obtains an energy

$$U = -\boldsymbol{\mu} \cdot \boldsymbol{B} \tag{3.1}$$

This energy differentiates an atom's various spin states which would otherwise have the same energy, i.e. "lifts the degeneracy". For example, considering an electron with only a spin (vs total angular momentum) magnetic moment:

$$\mu = -\frac{e}{2m_e} g_e S \tag{3.2}$$

in a field $\boldsymbol{B} = B\hat{z}$, the two spin states have energies separated by:

$$\Delta U = -\mu_B g_e B \tag{3.3}$$

This comes about because the spin 1/2 electron has $\hat{z}$ component spin eigenvalues $\pm\hbar/2$. Using the relationship between the energy and angular frequency (ω) of an electromagnetic wave $E = \hbar\omega$, we can relate the frequency of the applied wave to the energy gap by [14]:

$$\omega = \gamma B \tag{3.4}$$

where γ is the object's gyromagnetic ratio. By applying an electromagnetic field at a specific amplitude, or frequency, the particle can be caused to transition between, or "driven", between the two energy states.

The same process can be implemented for more complicated systems where more factors are taken into account such as the exploitation of nuclear spin states in NMR measurements.

3.2 Hyperfine Structure

The hyperfine atomic energy level splitting, or structure, is due to a collection of effects, predominantly the nuclear magnetic moment's interaction with the magnetic field of the orbiting electron(s). The large mass of the nuceons compared to that of an electron results in a splitting smaller than the *fine* structure by several orders of magnitude. The *hyperfine* splitting of atomic energy levels is on the order of $\alpha^2 m_e/m_p$, where α is the fine structure constant,and $m_{e,p}$ are the electron and proton masses [8]. The nuclear magnetic moment is related to the spin of the nucleons, $\boldsymbol{I}$, by:

$$\boldsymbol{\mu_I} = g_I \mu_N \boldsymbol{I} \tag{3.5}$$

where g_I is the g-factor of the nuclei, and μ_N is the nuclear magneton.

In the presence of a magnetic field the nuclear magnetic moment has an energy associated with it, $U = -\boldsymbol{\mu_I} \cdot \boldsymbol{B}$. The hyperfine interaction is brought about by coupling between the orbital $\boldsymbol{L}$, electron spin $\boldsymbol{S}$, and nuclear spin $\boldsymbol{I}$, angular momenta via the Hamiltonian:

$$H_{hf} = A_{hf} h \ \boldsymbol{J} \cdot \boldsymbol{I} \tag{3.6}$$

where $\boldsymbol{J} = \boldsymbol{L} + \boldsymbol{S}$ is the total electron angular momentum, h is Plank's constant, and A_{hf} is the hyperfine coupling constant [8]:

$$A_{hf} h = \frac{g_e \mu_I \mu_B}{I} \langle \frac{1}{r^3} \rangle \frac{l(l+1)}{J(J+1)} \tag{3.7}$$

where l is the electron orbital angular momentum quantum number and J is the electron total angular momentum quantum number. Note, if A_{hf} was zero, the Hamiltonian would not account for electron-nuclei interaction.

The Hamiltonian, neglecting Coulomb and spin-orbit interactions, for an atom immersed in a magnetic field ($\boldsymbol{B}_0$) is given by:

$$H = A_{hf} h \boldsymbol{J} \cdot \boldsymbol{I} - \boldsymbol{\mu}_J \cdot \boldsymbol{B}_0 - \boldsymbol{\mu}_I \cdot \boldsymbol{B}_0 \tag{3.8}$$

where ($\boldsymbol{\mu}_J = -g_J \mu_B \boldsymbol{J}$) [8]. The first term is the hyperfine interaction from (3.6), the second and third terms are the atom's valence electron and nuclear magnetic moments interaction with $\boldsymbol{B}_0$.

Equation (3.11) gives g_J. The eigenvalues of Hamiltonian are characterized by the quantum numbers F, and m_F, where $\boldsymbol{F} = \boldsymbol{I} + \boldsymbol{S}$, and $m_F = -F, -F+1, \cdots, F-1, +F$. The jargon for different F levels are "manifolds". Additionally, the nuclear spin quantum number is: I=5/2 for ^{85}Rb, and I=3/2 for ^{87}Rb, ^{39}K, and ^{41}K [4]. The natural abundance of ^{85}Rb is 72%, and ^{87}Rb is 28% [2].

The presence of the external magnetic field lifts the degeneracy in m_F. The energy, or frequency, of a particular hyperfine level (ground state) is given by the Breit-Rabi formula. Ignoring a small nuclear magnetic moment term, and taking the electron total angular momentum quantum number to be $J = 1/2$, and thus the total atomic angular momentum number to be $F_\pm = I \pm 1/2$ [2]:

$$E(F_\pm, m_F) = -\frac{\Delta E_{hf}}{2(2I+1)} \pm \frac{1}{2}\sqrt[2]{\Delta E_{hf}^2 + \frac{4m_F}{2I+1} g_J \mu_B B \Delta E_{hf} + (g_J \mu_B B)^2} \tag{3.9}$$

where ΔE_{hf} is the hyperfine energy splitting when *no* magnetic field is applied. I.e., the energy between the $F = 2$ and $F = 1$ manifolds:

$$\Delta E_{hf} = \eta \hbar^2 (I + 1/2) \tag{3.10}$$

where η is a constant that characterizes the magnetic interaction between the alkali metal nucleus and electrons, see [10]. For ^{85}Rb $\Delta E_{hf} = 3036$ MHz, and for ^{87}Rb $\Delta E_{hf} = 6835$ MHz. I, S, L, and J are the nuclear spin, electron spin, electron orbital angular momentum, and total electron angular momentum quantum numbers respectively. The g_J variable is the Landè g-factor of total electron angular momentum:

$$g_J = 1 + \frac{J(J+1) + S(S+1) - L(L+1)}{2J(J+1)} \tag{3.11}$$

For more information on the hyperfine structure of alkali atoms,including a discussion of the low-field derivative of the EPR frequency with respect to the applied field, see Jaideep Singh's PhD thesis page 667.

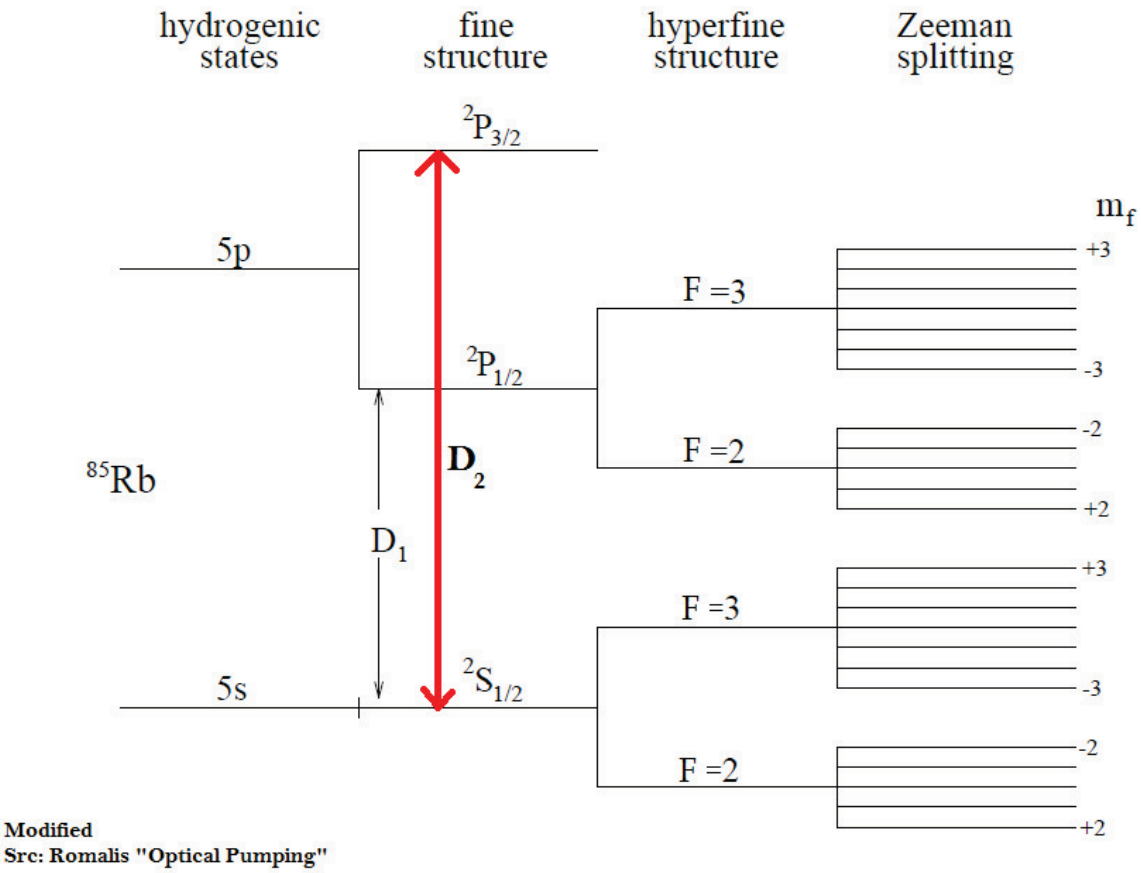

FIGURE 3.1: ^{85}Rb electron hyperfine energy level splitting with further Zeeman splitting on the right. Lines not to scale.

3.3 Contact Interaction

The hyperfine interaction is, for our purposes, dominated by the Fermi contact interaction. The interaction is a classical magnetostatic interaction of quantum mechanical entities, namely the ^{3}He nucleus and the alkali metal valence electron [11]. It is this dipole interaction that is responsible, via binary collisions, for the spin exchange between the optically pumped alkali metal electrons and the ^{3}He.

The interaction takes place when the alkali metal electron is located inside the nucleus, hence the name "contact". Only spherical $l = S$ states are affected because, unlike those with a higher l number, the wavefunctions (Ψ) of these electrons have no node at the center, and thus a non-zero probability of finding the electron. The ground state of an alkali metal electron is this $l = S$ state. Because the effect is the same in all directions, the other name for the interaction is the *isotropic* hyperfine interaction [1].

Throughout this paper, the nuclear spin of the alkali metal atoms will be denoted by $\boldsymbol{I}$, and that of the ^{3}He by $\boldsymbol{K}$. The previous choice of $\boldsymbol{I}$ for the nuclear spin in the discussion of the hyperfine structure, however, was arbitrary, as both the alkali metals and ^{3}He display hyperfine structure in their energy levels.

The interaction Hamiltonian is given by[12]:

$$H_{K,S} = -\frac{8}{3}\pi\langle\boldsymbol{\mu}_K \cdot \boldsymbol{\mu}_e\rangle|\Psi(R)|^2 = \frac{8}{3}\frac{(g_e\mu_B)\mu_K}{K}|\Psi(R)|^2\ \boldsymbol{K}\cdot\boldsymbol{S} \tag{3.12}$$

where $\boldsymbol{K}$ and $\boldsymbol{S}$ are the spins of the ^{3}He nucleus and alkali metal electron, $\boldsymbol{\mu}_K$ and $\boldsymbol{\mu}_e$ are the ^{3}He nuclear and alkali metal valence electron spin magnetic moments respectively, μ_B is the Bohr magneton, and $|\Psi(R)|^2$ is the probability of the alkali metal electron being found at the location of the ^{3}He nucleus (R is the helium-alkali metal interatomic distance). The above equation relies on the following relationship between the nuclear magnetic moment (μ_K), the nuclear g-factor (g_K), the nuclear magneton (μ_N), the nuclear spin (K):

$$\boldsymbol{\mu}_K = (g_K)\frac{\mu_N}{\hbar}\boldsymbol{K} = \left(\frac{\mu_K\hbar}{K\mu_N}\right)\frac{\mu_N}{\hbar}\boldsymbol{K} = \frac{\mu_K}{K}\boldsymbol{K} \tag{3.13}$$

Chapter 4

Polarization Process & Optical Pumping

4.1 Optical Pumping

We use the process of optical pumping to first polarize the alkali metal valence electrons. This technique uses circularly polarized laser light of an appropriate wavelength (795 nm) is used to get the alkali metal's valence electrons into the desired spin state via a transfer of angular momentum. For example, the laser light excites the electrons into a excited state ($5P_{1/2}$), from which they then decay with equal probability, due to collisional mixing, to either of the $5S_{1/2}$, $m_s = \pm 1/2$ states. These are all discrete processes that can only occur subject to quantum mechanical selection rules. The 1/2 state cannot be excited any further and remains as is, while the -1/2 state is re-excited. Over a period of time, the original energy levels of the alkali metal are thus "pumped, or repopulated into the desired ($m_s = +1/2$) state.

A similar process, with more absorption and decay steps, occurs for all the different m_F until the electrons reach a state from which they cannot be excited, typically the $m_F = \pm 3$ state. The final state depends on whether σ_+ or σ_- polarized light is used in the pumping. The sign of σ is determined by whether the photons carry positive, or negative, angular momentum with respect to the direction of B_0 [10]. A transition of $m_F \rightarrow m_F \pm 1$ is brought about by absorption of $\pm\sigma$ light.

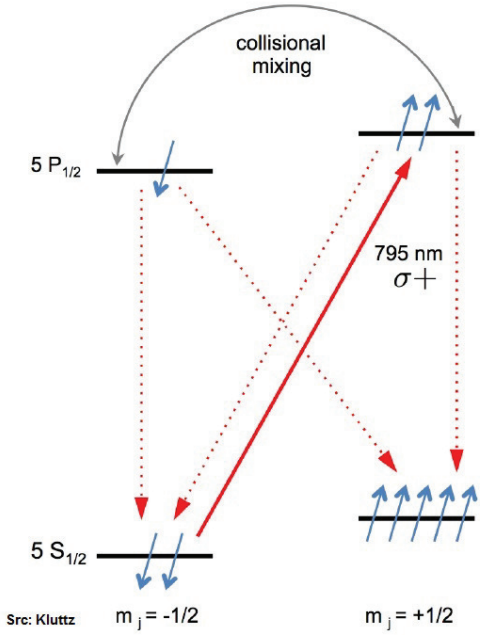

FIGURE 4.1: Optical pumping transitions.

Our lasers can only directly pump the Rb inside the target because of the narrow energy gap between the $5P_{1/2}$ and $5P_{3/2}$ levels of K [1]. Thus the desired quanta of spin angular momentum propagates from the lasers to the Rb, to the K, which then transfers it to the ^{3}He. The K$\leftrightarrow$Rb, and K$\leftrightarrow$ ^{3}He transfer occurs via collisions, and known in the field as "spin-exchange".

The N_2 in the targets acts, via collisions, to absorb energy from excited alkali metals. The diatomic N_2's many degrees of freedom take up energy that would otherwise be reradiated as photons. These random photon emissions would be detrimental to the polarization of the target, and the N_2 "quench" their effect.

The targets will depolarize in the absence of external interference. The jargon for this is relaxation, i.e. returning to an equilibrium state from which the spin was excited. Thus the polarization process is ongoing in our lab while we study the targets, and while the experiments are up and running.

4.2 AFP

Adiabatic Fast Passage (AFP) is an technique, used here to reverse the ^{3}He spins' direction, and thus that of the bulk magnetized ^{3}He, by 180°. Recall that spin is proportional to the magnetic moment of the nuclei. These nuclear moments sum to a bulk magnetization of the ^{3}He gas as a whole. This macroscopic moment precesses about B_0 in the, stationary, reference frame of the

lab. The bulk 180° rotation of the spins puts the magnetization parallel or antiparallel to the holding field. Afterwards, the alkali metals are subject to a field:

$$\boldsymbol{B}_{tot} = (\boldsymbol{B}_{\boldsymbol{se}} + \boldsymbol{B}_{\boldsymbol{M}}) \pm \boldsymbol{B}_{\boldsymbol{0}} \tag{4.1}$$

Both EPR and NMR utilize the AFP rotation of the nuclear spins. NMR is a technique used to measure the *relative* ^{3}He polarization.

AFP is a set of conditions under which we rotate the spins quickly (fast) compared to their relaxation times, but slowly enough (adiabatic) that they can follow the magnetic field that brings about the rotation, described below.

The holding magnetic field B_0 is what aligns the ^{3}He spins along the axis of the laser, conventionally designated $\hat{z}$. This alignment means a mixture of parallel and antiparallel states, not polarization. The ^{3}He nuclei have a magnetic moment $\boldsymbol{\mu_K} = \gamma \boldsymbol{K}$, due to their angular momentum, $\boldsymbol{K}$. When immersed in a magnetic field, a torque $\boldsymbol{\tau}$ is exerted on the nuclei. The work done by this torque changes the direction of $\boldsymbol{K}$. The result is precession of the moment about the total applied field, like a spinning top going around the vertical because of gravitational torque, while still rotating about its axis.

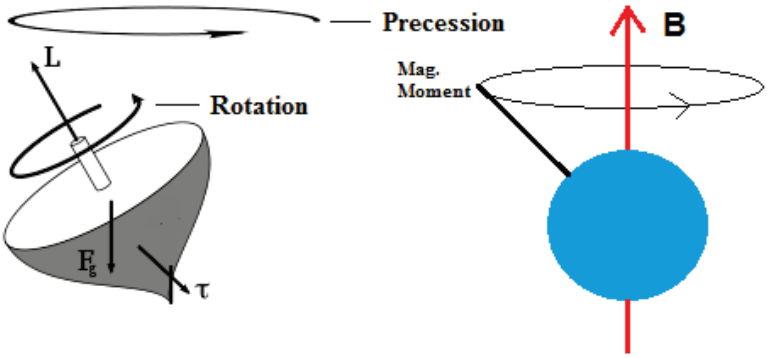

FIGURE 4.2: Precession in a spinning particle, and top.

$$\boldsymbol{\tau} = \frac{d\boldsymbol{K}}{dt} = \boldsymbol{\mu_K} \times \boldsymbol{B_0} \tag{4.2}$$

$$\frac{d\boldsymbol{\mu_K}}{dt} = \gamma \boldsymbol{\mu_K} \times \boldsymbol{B_0} \tag{4.3}$$

where γ is the gyromagnetic ratio, 3.243 KHz/G for ^{3}He [1].

4.2.1 Rotating Frame - Effective Field

A way to visualize the AFP magnetization rotation is by adopting a reference frame, denoted with primes, rotating at the frequency $\boldsymbol{\omega_{RF}} = \omega_{RF}(-\hat{z})$. As outlined in [14] pages 49-50, this is done by adopting the coordinate transformation:

$$\left.\begin{aligned} \hat{z}' &= \hat{z} \\ \hat{x}' &= \cos(\omega_{RF}t)\hat{x} - \sin(\omega_{RF}t)\hat{y} \\ \hat{y}' &= \sin(\omega_{RF}t)\hat{x} + \cos(\omega_{RF}t)\hat{y} \end{aligned}\right\} \tag{4.4}$$

As derived in Taylor's *Classical Mechanics*, the vector transformation of a time derivative of a general vector $\boldsymbol{Q}$ in a frame rotating at ω_{RF} is:

$$\frac{d\boldsymbol{Q}}{dt}_{stationary} = \frac{d\boldsymbol{Q}}{dt}_{rotating} + \boldsymbol{\omega_{RF}} \times \boldsymbol{Q} \tag{4.5}$$

Using this the rate of change of the magnetic moment in the rotating frame can be written as:

$$\begin{aligned} \frac{d\boldsymbol{\mu_K}}{dt}_{rotating} =& \frac{d\boldsymbol{\mu_K}}{dt}_{stationary} - \boldsymbol{\omega_{RF}} \times \boldsymbol{\mu_K} \\ =& \gamma\boldsymbol{\mu_K} \times \boldsymbol{B_0} + \omega_{RF}(\hat{z} \times \boldsymbol{\mu_K}) \\ =& \gamma\boldsymbol{\mu_K} \times (\boldsymbol{B_0} - \frac{\omega_{RF}}{\gamma}\hat{z}) \\ =& \gamma\boldsymbol{\mu_K} \times \boldsymbol{B_{eff}} \end{aligned} \tag{4.6}$$

The ^{3}He nuclear spins precess at the Larmor frequency, $\omega_0 = \gamma B_{eff}$, about the equivalent field, $\boldsymbol{B_{eff}} = B_0 - \frac{\omega_{RF}}{\gamma}\hat{z}$, in the rotating frame. The effective field is what the ^{3}He magnetization follows in its (AFP) reversal of direction.

4.2.2 Addition of RF Field

When an oscillating RF field B_1 is applied at angular frequency ω_{RF}, perpendicular and in addition to B_0, the 180° rotation ($\pm\hat{z} \rightarrow \mp\hat{z}$) can be brought about by sweeping either the holding field magnitude, or the frequency ω_{RF}. In the rotating reference frame, B_{eff} is described by:

$$\boldsymbol{B_{eff}} = (B_0 - \frac{\omega_{RF}}{\gamma})\hat{z}' + B_1\hat{y}' \tag{4.7}$$

The Larmor frequency is this frequency of the rotating frame and also the RF frequency applied to rotate the spins.

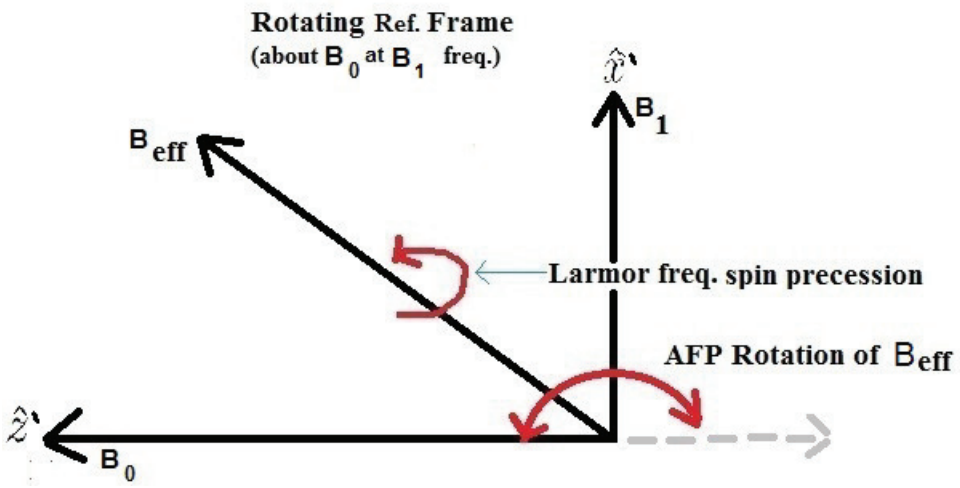

FIGURE 4.3: Fields, rotation, and precession.

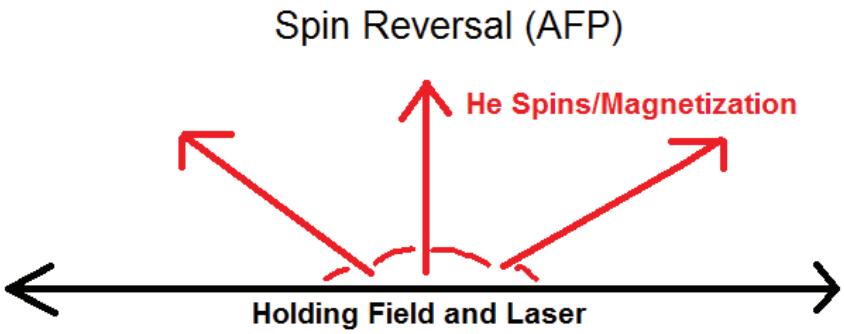

FIGURE 4.4: APF 180° spin reversal

4.2.3 NMR

NMR exploits Zeeman splitting due to nuclear magnetic moments interacting with an applied magnetic field. The process is similar to driving electron energy level transitions, where now it is the nuclei that are transitioning between energy levels. For example, when $B_0 = \omega_{RF}/\gamma$, $\boldsymbol{B_{eff}}$ is oriented solely in $\hat{x}$, perpendicular to the holding field. This is the resonance condition used in NMR to flip the spins of the ^{3}He nuclei between energy levels, and is the condition for maximum NMR signal [1].

To clarify, there are two types of spin reorientation which take place. First,the quantum scale spin flipping of the ^{3}He nuclear spins and alkali metal electrons, second, the bulk macroscopic rotation of the ^{3}He magnetization. This is potentially confusing because EPR utilizes the AFP

NMR technique and apparatus to flip , and rotate, the spins of the helium. However, the EPR data signal comes from the alkali metal light emissions, whereas that of the NMR is from a coil-induced *emf* from the magnetized ^{3}He.

A sample NMR sweep is shown below. The peaks give the relative amplitude. The signal is plotted, then fit using:

$$S(t) = M \cdot \frac{B_1}{\|B_{eff}\|} = M \cdot \frac{B_1}{\sqrt{(B - B_0)^2 + B_1^2}} + aH + b \tag{4.8}$$

where the signal is proportional to the component of the magnetization perpendicular to $\boldsymbol{B_0}$. The peak height, M, from this fit is proportional to the ^{3}He's relative polarization, so a difference in heights indicates a loss. One peak is the magnetic field "upsweep" (increased through resonance) and the other is the "downsweep". They should both be maximum at the same magnetic field strength. That they are not is an artifact of the electronics.

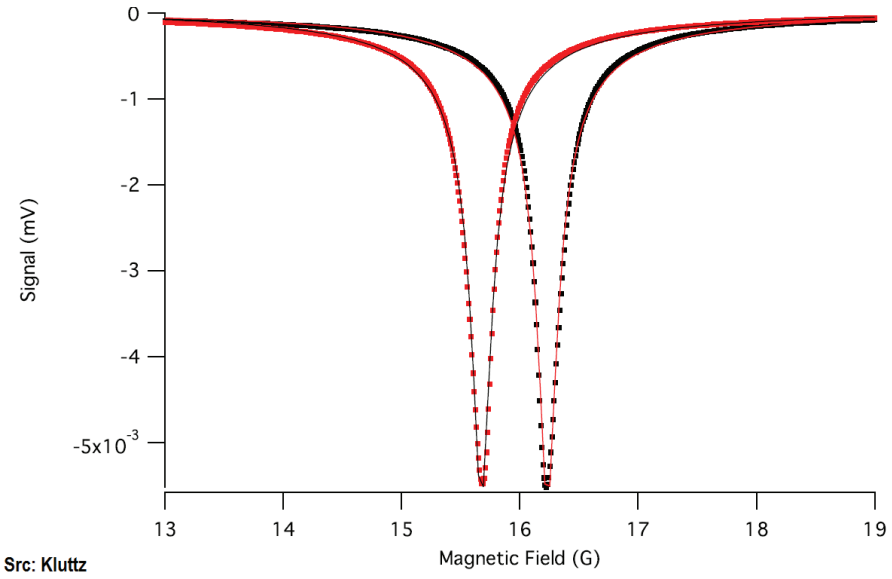

FIGURE 4.5: Example of NMR scan data used to gauge the helium polarization.

4.3 EPR

We use the technique of Electron-Paramagnetic-Resonance (EPR) in measuring the ^{3}He's polarization, and in detecting the frequency between the m_F levels. This involves the application of yet another oscillatory magnetic field, with a frequency in MHz, via another pair of coils. These are the EPR$_{RF}$ field and coils respectively.

The EPR_{RF} field's frequency (FM-frequency modulated EPR), or field strength (AM-amplitude modulated EPR), can be varied to obtain the signal we desire. For the κ_0 studies, we will be using FM-EPR, varying the frequency until we observe emissions corresponding to a specific energy level transition ("D_2") in the alkali metal we wish to examine. In Rb, this light corresponds to the $5P_{3/2} \rightarrow 5S_{1/2}, \lambda = 780\text{nm}$ transition.

We search for the EPR_{RF} frequency for which maximum D_2 light is emitted. This indicates that we are driving alkali metal valence electrons out a particular energy state (m_F). This is a hyperfine energy level splitting, involving the electrons' interaction with nuclear spins, and thus is dependent upon which alkali metal isotope is being used. During EPR, the EPR_{RF} field is applied throughout to drive the transitions.

Using D_2 light as an indicator of driving m_F levels is an indirect method. Optical pumping polarizes the majority of the alkali metal valence electrons into a particular m_F level (see above). If this level is 100% populated, there are no D_2 emissions. The EPR_{RF} field destroys this polarization exciting electrons out of the polarized state. Collisions further excite some electrons to the higher states, whereby their decay emissions (D_2) are observed. Put simply, a peak in D_2 emissions tells us that we have driven the electrons out of the state they would otherwise be in. The EPR_{RF} frequency necessary to excite an electron from that state, is then proportional to the energy gap between the states. We typically drive the $m_F = -3 \rightarrow m_F = -2$ transition.

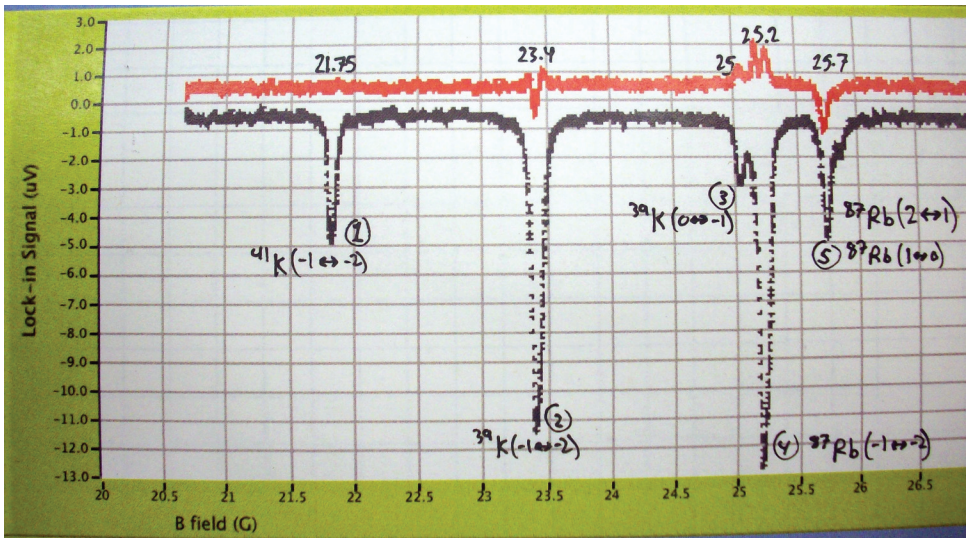

FIGURE 4.6: Example AM-EPR sweep data used to show the various alkali transitions avaliable to measure. Note that some peaks contain multiple unresolved transitions, and that some peaks are too far to the left or right to be seen.

Knowing the condition to apply to drive the transitions means we also have found the levels' energy difference. We know what the energy difference should be under the influence of our

applied holding field, so the deviation from that is due to the magnetization, and thus polarization, of the ^{3}He. Because of the deviation, this type of EPR is called "frequency-shift" EPR. To isolate the ^{3}He's contribution to the splitting, we use frequency shift AFP rotation process described above. By sweeping the frequency of the applied RF field B_1 we reverse the ^{3}He's magnetization with respect to the holding field. This causes a change in the transition frequency which the EPR electronics follow. Knowing the splitting when the ^{3}He is aligned, then anti-aligned to B_0, allows this isolation.

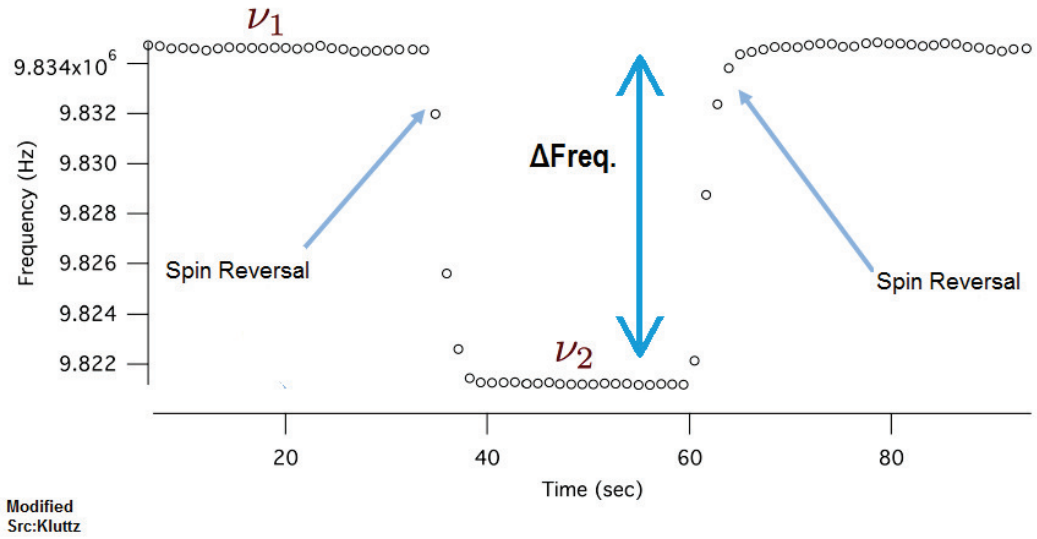

FIGURE 4.7: Sample FM-EPR data signal. The trough corresponds to a change in the resonant (maximum D_2) frequency due to bulk reversal, via AFP, of the ^{3}He spins. The vertical axis is the resonant EPR$_{RF}$ frequency.

4.3.1 Obtaining the ^3He Polarization

Typically, NMR sweeps are used as a relative polarization gauge of both signal quality and magnitude.

Assuming the EPR frequency ν exhibits small variations with respect to the applied magnetic field we can use (k0 section eqn for derivative) to solve (eqn for deltafreq) or a variant corrected for nonspherical target geometry for P, the ^{3}He nuclear polarization.

The derivative can be expresses, to lowest order by [1]:

$$\frac{d\nu_{F,m_F}}{dB} = \frac{\mu_B g_e}{h(2I+1)} \tag{4.9}$$

As outlined in [16], the full low-field derivative can be expressed as:

$$\frac{d\nu}{dB} = \mp\frac{g_I\mu_N}{h} + \frac{g_I\mu_N - g_s\mu_B}{2h[I]}\left(\frac{2m_F + [I]x}{\sqrt{1+\frac{4m_F}{[I]}x+x^2}} - \frac{2m_F - 2 + [I]x}{\sqrt{1+\frac{4(m_F-1)}{[I]}x+x^2}}\right) \tag{4.10}$$

where $[I] = 2I + 1$, g_s is the electron g-factor and:

$$x = (g_I\mu_N - g_s\mu B)\frac{B}{h\nu_{hfs}} \tag{4.11}$$

$$h\nu_{hsf} = \frac{A_{hfs}[I]}{2} = \Delta E \tag{4.12}$$

where the latter is the hyperfine energy splitting in the presence of *no* applied magnetic field.

Chapter 5

Apparatus

5.0.2 Apparatus

Below is a simplified schematic of the previous experimental apparatus without the optics or electronics. The experiment to measure κ_0 modified the lab's previous setup, while remaining similar in fashion. The holding field ($\boldsymbol{B_0}$) of approximately 10G to 30G is generated by the main Helmholtz coils. This field,($\boldsymbol{B_0}$), is parallel to the direction of propagation of the primary laser. N. Penthorn constructed the current κ_0 measurement apparatus over the summer of 2013. The main changes were the construction of the rotating cell-oven, polarizing optics, and the filling of the cylindrical cells. Now the apparatus utilizes two laser sources, a primary and probing laser. The primary laser is used to polarize the cell prior to measurements being made. The probing laser pumps the cell at 45 deg to $\boldsymbol{B_0}$ during measurements. We used broadband (FAP) lasers, and a QPC brand narrowband laser to pump the alkali with light of wavelength 794 nm, and power of about 27 W.

The optics not only circularly polarize the light,they include a cylindrical lens to shape it. This attempts to maximize the amount of light incident on the cell. These simple optics are as follows. A Polarizing beam splitter (PBS) splits the incident beam into two linearly polarized beams leaving the cube perpendicular to each other. One is sent to a dump, to safely collect the unused laser light, the other passes through a quarter wave plate ($\lambda/4$). Passing through the plate introduces a $\pi/2$ phase difference between the light's electric and magnetic field components, i.e. it circularly polarizes the light. The cylindrical lens then follows.

The cell "Symon" is 8 inches in length, has an outer diameter of 0.5 inches, an inner volume 12.88 ml, and was filled with a Rb-K mixture and 7.97 amagats of ^{3}He. Symon was found to have a lifetime of approximately eighteen hours, with the pumping lasers off, and the heaters on.

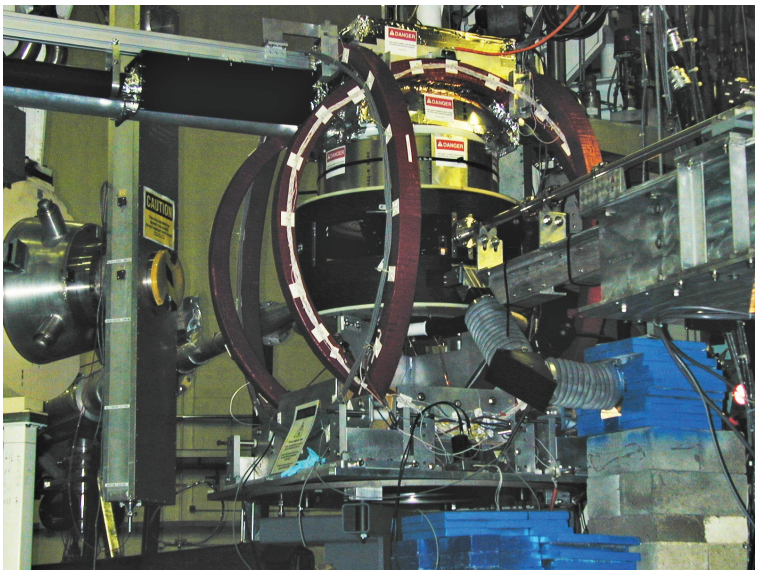

FIGURE 5.1: [3] Target enclosure at the TJNAF (JLab). Various magnetic field coils are visible.

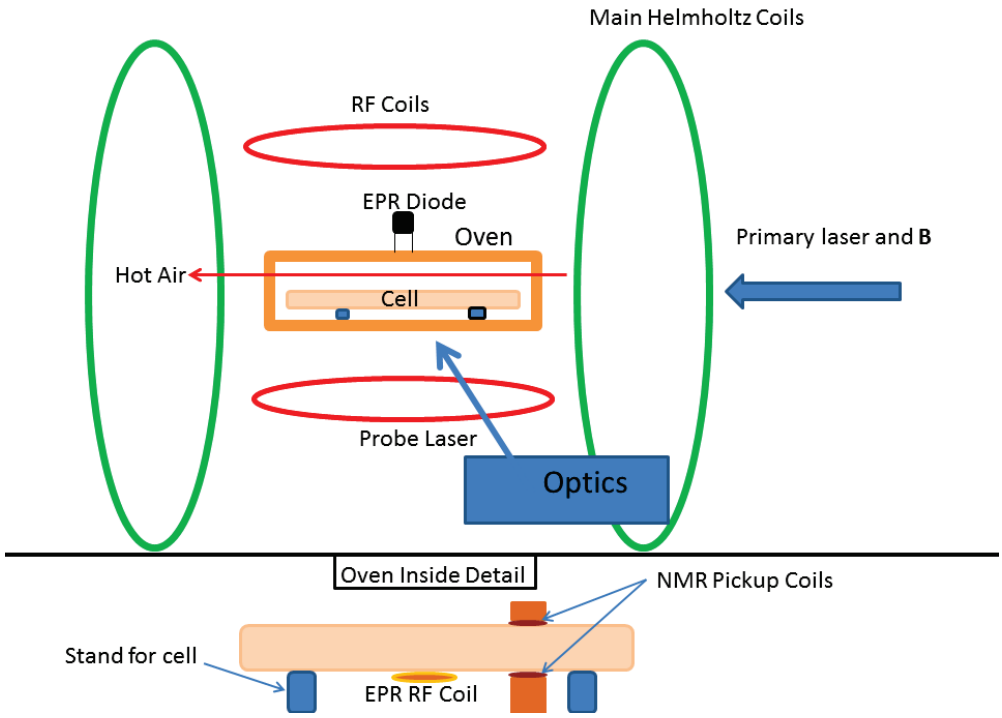

FIGURE 5.2: The main (green) coils produce the holding field ($\boldsymbol{B_0}$)and the red make the RF ($\boldsymbol{B_1}$). The ^{3}He target is enclosed in a forced-air oven in the center with various additional coils surrounding it.

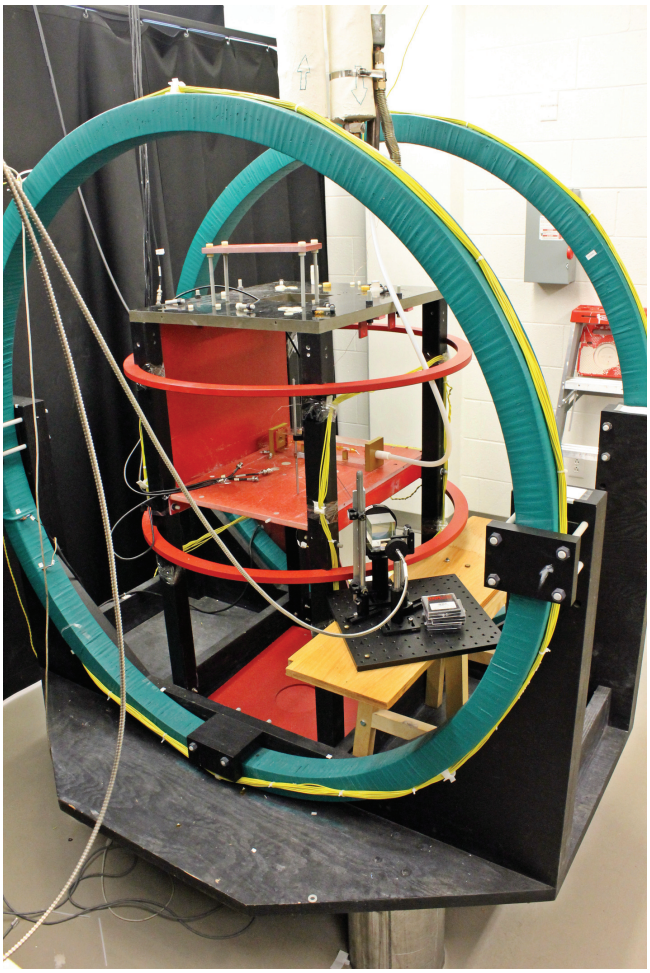

FIGURE 5.3: Side view of the primary apparatus, including coils, main experimental table on which the oven rests, and the polarizing optics for the probing laser.

5.0.3 κ_0 Oven

To measure the EPR frequencies, the experimental setup is similar in nature to that already in use in the lab, as described above. The primary difference being that the target must now be able to be rotated with respect to the holding field. A cylindrical cell approximately 20cm long and 2cm in diameter was ordered from a glassblower. The cell was filled a small amount of Rb and K, then N_2 and ^{3}He. Next, a glass, forced-air, oven to contain and heat the cell was constructed. The oven may not contain any ferrous metal, which would interfere with the various magnetic fields. It must also have a long, transparent side so that the pumping lasers can illuminate the cell sufficiently.

For these reasons we chose to construct the oven from length of square glass tubing, with high temperature plastic end caps. The experimental cylindrical cell rests on blocks, secured with

RTV silicon, inside the square glass tube. The end caps have a square channel machined in them to accommodate the glass tube. Threaded through-holes in the end caps, along the axis of the tubing, allow hot air to enter the oven. A hose attachment was added to secure Teflon tubing to the oven. The Teflon tubing carries forced air at 235°C to, and away from, the oven. Further small through holes accommodate temperature sensors (thermocouples), and the wires from the NMR pickup coils. The bottom of both end caps have a peg, so the process of changing the cell orientation is repeatable. When the orientation is changed, the entire oven is lifted off of the table, turned 45°, and the pegs set back down into holes.

To keep the laser illumination at the cell constant for both orientations, the probing laser is oriented at 45° to the cell and oven, in the plane of the tabletop that the apparatus rests on. EPR RF field coils are attached to the bottom of the oven, perpendicular to the holding field, and above cylinder's cylinder. The NMR pickup coils form a "C" shape above and below the cell. A photodiode is positioned above the cell directly above the EPR RF coils, to receive the alkali metal fluorescence signal.

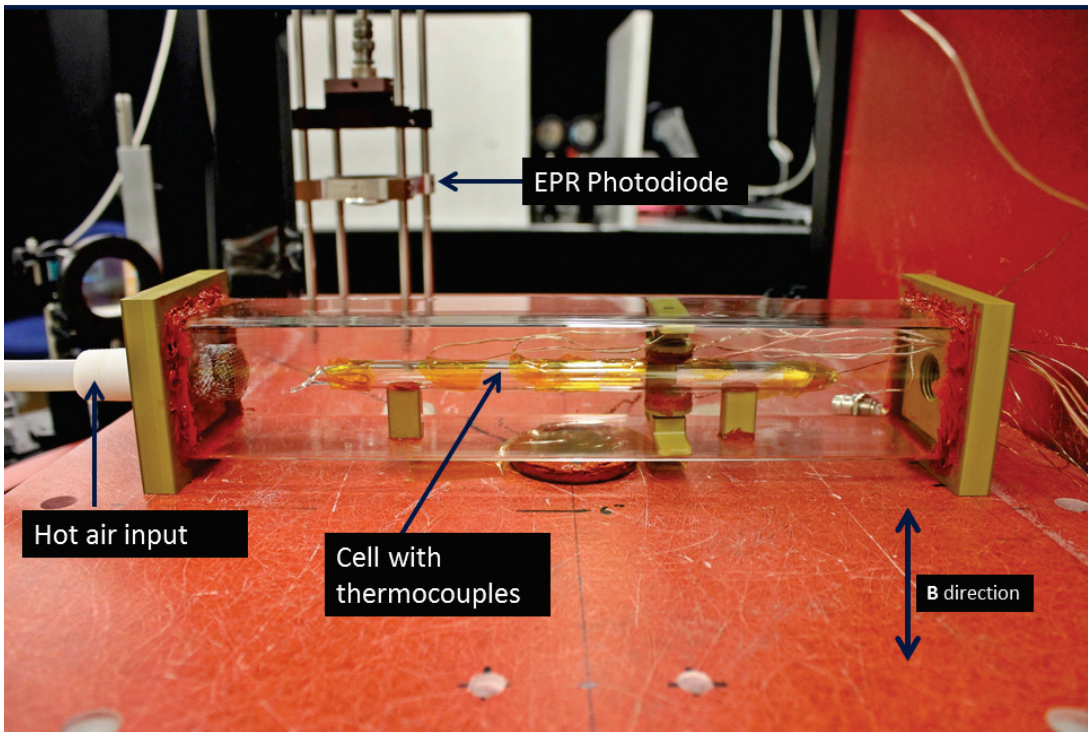

FIGURE 5.4: Picture of the oven, cell, and experimental table inside the main and RF coils. Note that the oven in is pictured in the perpendicular orientation.

Chapter 6

Data

6.1 Previous Groups Values

From Babcock et al. we have the following plot of data for the κ_0 of various alkali metals. This group accounted for polarization losses between frequency measurements by normalizing the shifts to NMR free induction decay amplitudes, a relative measure of polarization. As the value of κ_0 for Rb has been extensively determined, taking the ratio of measured frequency shifts allowed:

$$\kappa_{0,K} \propto \frac{\Delta\nu_K}{\Delta\nu_{Rb}}\kappa_{0,Rb} \tag{6.1}$$

to determine $\kappa_{0,K}$ over a range of temperatures. Testing the linearity of the dependence of κ_0 on temperature was a goal of our experiment, however, at the time of writing, there was not enough data to make a conclusion.

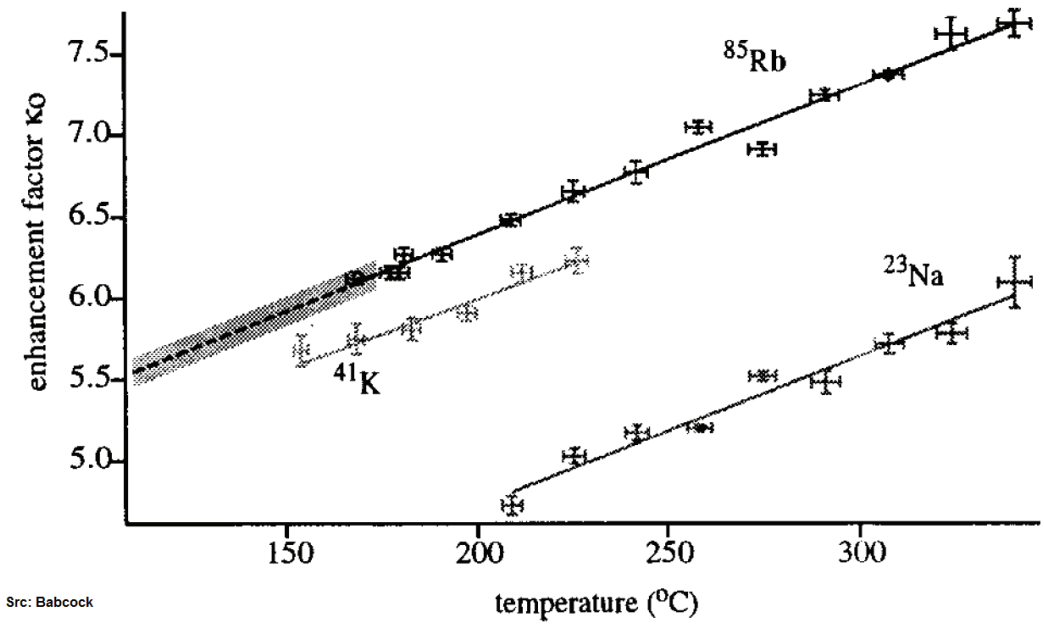

FIGURE 6.1: Experimental data from Babcock plotting κ_0 vs temperature. Top line ^{85}Rb, Middle ^{39}K, Bottom ^{23}Na. Shaded, dotted, line is data from Romalis and Cates. [5]

6.2 Our Work and Results

To begin measurements, we start with the standard procedure for EPR scans. An FM EPR sweep is performed to gauge the frequency of the alkali hyperfine transition we wish to measure. We then manually find the resonant frequency with the lock-in amplifier, and turn on the electronic feedback to "lock" the system to that transition.

We established a data taking procedure of turning on the EPR RF, waiting for a appreciable "plateau" to be recorded, flipping the spins (AFP), taking an NMR polarization measurement, turning off the EPR RF and lasers, reorienting the cell, then repeating. The lasers were off during the physical cell reorientation for safety, and the EPR RF turned off to minimize polarization losses. The reorientation took approximately two to three minutes, during which the entire glass oven was changed from being parallel to perpendicular to the axis of the holing field. The EPR photodiode was removed, then replaced, during each reorientation.

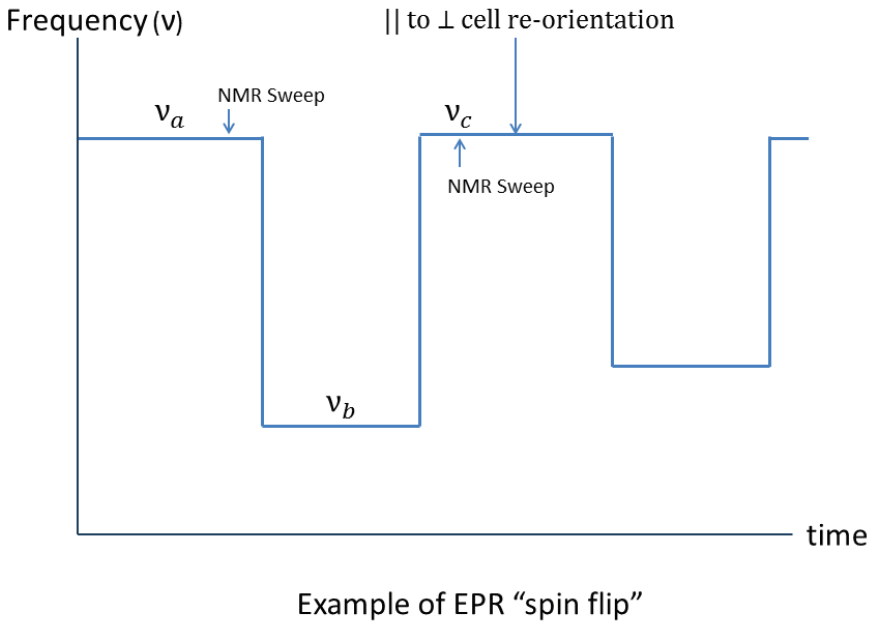

FIGURE 6.2: Plot showing two example "spin flips". Between five and ten of these flips were performed for each measurement of a particular alkali species and isotope.The differences in frequency between the top and "trough" are the desired frequency shifts.

Using this we took frequency shift data for a number of different alkali,isotope,temperature combinations. Each frequency (ν_a, ν_b, ν_c was found via a linear fit of that section of the data. The average of the frequency shift before and after the flip is what is being recorded as $< \Delta\nu >$. The average is weighted by the uncertainties from the linear fit.

6.2.1 Results

The cleanest data were obtained for the ^{41}K ($0 \leftrightarrow 0$) transition, indicated in the first row of the following table. In this table only the first perpendicular and parallel frequency shift are recorded. These were then used to calculate κ_0. Note that, while the expected order of magnitude, these are preliminary results and work is still ongoing to correct for systematic and statistical uncertainties. In particular, as described in the next section, there are polarization losses inherent in each frequency shift measurement that could potentially introduce large fluctuations in these data. For example, the polarization independence of (2.10) does not hold; the polarization does not cancel.

Species	^{41}K	^{39}K	^{39}K	^{39}K	^{87}Rb
Transition	(0 to 1)	(-1 to -2)	(-1 to -2)	(-1 to -2)	(-1 to -2)
Temperature	T = 210 C	T = 195 C	T = 198 C	T = 210 C	T = 194 C
$\langle\Delta\nu\rangle_\perp$ (MHz)	0.01655	0.01160	0.01660	0.02645	0.01060
$\langle\Delta\nu\rangle_\perp$ Uncertainty	4.3730E-05	4.5012E-05	3.6628E-05	3.5771E-05	5.4278E-05
$\langle\Delta\nu\rangle_\parallel$ (MHz)	0.01847	0.01339	0.01819	0.02875	0.01177
$\langle\Delta\nu\rangle_\parallel$ Uncertainty	4.4149E-05	5.2239E-05	2.5416E-05	3.1583E-05	5.1448E-05
κ_0	6.7148	5.1103	8.0802	8.8750	7.0449
κ_0 Uncertainty	0.2216	0.2001	0.2340	0.1878	0.4602

TABLE 6.1: Preliminary calculated values. κ_0 calculated *without* correcting for polarization losses. **Statistical** uncertainties given above.

Appendix A contains a brief compilation of reported κ_0 values from various groups.

6.2.2 Uncertainties

As alluded to in the above section, there are polarization losses inherent in each frequency shift measurement. The exact cause of these "AFP losses" are an active area of research, but come they come about every time the ^{3}He's magnetization direction is reversed. This is the reversal used to flip the spins in EPR, and also in NMR. The NMR data taken with every spin flip are intended to be used as the reference to which the polarization is normalized. Then subsequent measurements will have the polarization corrected to account for the losses. This work is in progress at the time of writing. The AFP losses were measured to be 0.76% per spin flip. Thus in the calculation of κ_0 each of the frequency shifts is uncertain by 1.52%.

That there are systematic shifts, occurring is evident in the frequency shifts not being the same for successive measurements. This can be seen in the following plot, where the frequency shift is decreasing. It would be expected to constant if there were no polarization loss. The frequency shift is plotted against the EPR measurement number (sample number). These data are for the ^{4}1K, $(0 \leftrightarrow 1)$ transition.

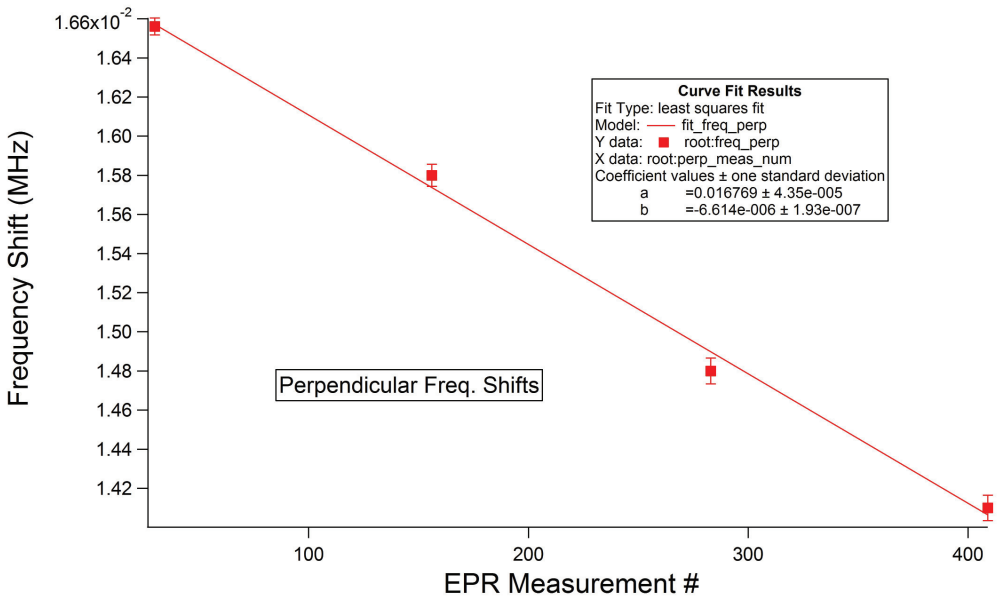

FIGURE 6.3: Plot showing the decrease in frequency shift of ^{4}1K, $(0 \leftrightarrow 1)$ due to polarization decreases with successive measurements.

Also regarding polarization, we noticed that rotating the cell, without any AFP occurring, caused a polarization loss of between two and four percent. Thus, the combined polarization losses per spin flip can be estimated at about 4%.

Another factor introducing a systematic uncertainty was that the frequency shift was found to be dependent on the position of the photodiode above the cell. This is estimated to introduce a 2500 Hz uncertainty in $\Delta\nu$, about $\pm 6.5\%$ of the typical $\Delta\nu \approx 0.02$MHz.

Another concern was that pumping the alkali with the spins anti-parallel to the holding field would cause losses in polarization. These losses were observed to be 1.2 Hz per second of opposite-direction pumping; negligible against the approximately 10-20KHz EPR frequency.

6.2.3 Temperature Studies

With the hot air blowing in on one end of the cell, that end was hotter than the output side. Because we were concerned that this temperature gradient would affect the data, we measured it with a series of six thermocouples attached to the outside of the cell. We consistently found a gradient of approximately $20°C$ from one end to the other. We made a Torlon baffle to stop the air from blowing directly on the tip of the cell, but this made no measurable difference in the gradient. Efforts to reduce the gradient were put aside afterwards for the duration of this senior project.

6.3 Conclusion

We have constructed an experimental apparatus to measure the spin exchange exchange constant κ_0. Preliminary values of κ_0 have been found for a variety of transitions for both Rb and K. These values are subject to large uncertainty, and systematic errors due to the loss of polarization with each measurement.

6.3.1 The Way Forward

There is much important information remaining to be determined for κ_0 measurements to be made more accurate. The first step should be to correct for the polarization losses, then recalculate the frequency shifts and thus κ_0. NMR measurements could be used to normalize the polarization to the pre-AFP value. Also, more data is needed for each transition and alkali isotope to reduce statistical uncertainties.

Finally, the behavior of κ_0 at different temperatures, and the effects of temperature gradients along the cell, need to be explored further.

I entered the lab for the first time in the summer of 2012, full of questions. I will leave the lab with a great deal more knowledge, experience, and still more questions.

Bibliography

[1] K. Kluttz, "Studies Of Polarized and Unpolarized ^{3}He In The Presence Of Alkali Vapor". Ph.D. Thesis, The College of William and Mary (2012).

[2] M. Romalis, "Optical Pumping of Rubidium Vapor.", Teaching Lab Manual. Revised Feb. 2009

[3] M.V. Romalis, G. D. Cates,Phys. Rev. A **58**, 4 (1998).

[4] Xiaochao Zheng, "Precision Measurement of Neutron Spin Asymmetry A_1^n at Large x_{Bj} Using CEBAF at 5.7 GeV.", Ph.D. Thesis, Massachusetts Institute of Technology, December (2002).

[5] E. Babcock et al., Phys. Rev. A **71**, 013414 (2005).

[6] A. S. Barton et al., Phys. Rev. A **49**, 4 (1993).

[7] A. Ben-Amar Baranga et al., Phys. Rev. Lett. **80**, 13 (1998).

[8] "Effects of the Nucleus on Atomic Structure.", M.I.T. Department of Physics, 8.421 Spring (2006). Web.

[9] "$G^n{}_E$ at High Q^2 E02-013 Experiment Homepage.", TJNAF Hall-A. jlab.org. Modified March (2006). Accessed April (2013). Web.

[10] R. Benumof, Am. J. Phys. **33**, 151 (1965).

[11] M. Bucher, Eur. J. Phys **21**, 19-22 (2000).

[12] T. Walker, W. Happer, Rev. Mod. Phys., **69**, 2, Apr. (1997).

[13] T. Walker, Phys. Rev. A, **40**, 9, (1989).

[14] P. Dolph, "High-Performance Nuclear-Polarized ^{3}He Targets for Electron-Scattering Based on Spin-Exchange Optical Pumping". Ph.D. Thesis, The University of Virginia (2010).

[15] J. R. Talyor, *Classical Mechanics* (University Science Books, 2005)

[16] J. Singh, "Alkali-Hybrid Spin-Exchange Optically-Pumped ^{3}He Targets Used for Studying Neutron Structure". Ph.D. Thesis, University of Virginia (2010).

Appendix A

Group	κ_0 Alkali Metal	κ_0 Value	Uncertainty	Temperature	Source
Romalis	Rb	4.52+0.00934 [T(°C)]	1.50%	110-172 °C	[3]
Barton	Rb	5.13 ±0.13	2.50%	74.5 °C	[6]
Romalis/Cates	Rb	6.39+0.00934[T-200(°C)]	1.5%	120-175(°C)	[5]
Babcock	K	5.99±0.11[T-200°C]	1.80%	200°C	[5]
Baranga	K	Kκ_0=0.94± 0.01· Rbκ_0	1%	Unclear (110-200°C)	[7]

Compilation κ_0 values found by other groups. Note, none explicitly stated corresponding alkali isotope and transition.